Analysis of a reversible flight control system response to atmospheric turbulence

K. Raissi, M. Mani, H. Ghaffari, A. Nobari
Department of Aerospace Engineering and Center
for Excellence in Computational Aerospace Engineering
Amirkabir University of Technology
Tehran, Iran

ABSTRACT

A mathematical model was developed for the reversible longitudinal control system of a regional commuter aircraft using the available geometry, mass property and kinematics. The model was incorporated into a general multi-body dynamics code and validated using existing manufacturer's data as well as recorded data from several flights. Analysis of the flight data revealed light atmosphere turbulence level. To investigate the effect of higher turbulence intensity on the reversible flight control system, a sever turbulence level was generated using Von Karman model for the same flight level and velocity. The result was used as a random input to the dynamic model for computation of the frequency response of control column. It was shown that turbulence could act as a random input through the hinge moment during the flight and introduced a new mode in the lower end of power spectral density curve. The energy induced by this low frequency input resulted in large displacement of control column in simulation which surpassed the existing limits. Therefore it should be taken into account when dealing with handling quality as well as autopilot design.

NOMENCLATURE

A	cable cross section
$\bar{c}$	mean aerodynamic chord
$\bar{C}_E$	elevator reference chord
C_h	elevator hinge moment coefficient
E	modulus of elasticity
g	the algebraic constraints
GE	ground effect
HM	aerodynamic hinge moment
l	chord length of the cable
m	mass per unit length of cable
$\mathbf{M}$	the positive definite mass matrix
n	number of degrees of freedom
q	generalised co-ordinates
$\bar{q}_H$	dynamic pressure
S_E	elevator area
T	cable tension
TT	trim tab
u	generalised velocities
V	aircraft velocity
w	turbulence vertical velocity
X_n	control column deflection
$\dot{Z}$	aircraft centre of mass vertical velocity
α	angle-of-attack
β	sideslip angle
ϕ	aircraft bank angle
θ	aircraft pitch angle
η	elevator deflection
λ	the Lagrange multipliers
σ	ground effect influence factor

Paper No. 3167. Manuscript received 6 February 2007, revised 4 October 2007, accepted 17 January 2008.

https://doi.org/10.1017/S0001924000002025 Published online by Cambridge University Press

Table 1.
Aircraft specification

Passenger	50
Wing span	15·2m
Wing area	52·5m^2
Gross weight	21,150kg
Engine type	2 × 2,800hp
Service ceiling	9,150m
Max speed	410km/h

Table 2
Available recorded data from scheduled flight

Flight No	Altitude (m)	Speed (km/h)	Weather
1	5,400	330	clear sky
2	5,100	340	clear sky
3	4,500	360	clear sky

1.0 INTRODUCTION

When an aeroplane passes through turbulent atmosphere, the first thing that occurs is an oscillating heave motion of the vehicle due to vertical velocity component of turbulence. This not only makes the crew and passengers uncomfortable, but induces an undesirable load factor to the aircraft structure. For these reasons, many studies have been conducted on this subject. However, a change in vertical velocity can change the flow field around the tail as well. This change can, in turn, alter the pressure distribution and cause the variation of hinge moment on the elevator. Since no one, to the authors' knowledge, had paid attention to this point, a research project was initiated to investigate it. The present paper outlines the efforts made toward an understanding the phenomenon and its effect. For this purpose data were collected from a commuter aircraft (Table 1) and its flight (Table 2). Since the aeroplane flight control system was reversible, the characteristics of such system had to be incorporated into the model. The first part of this paper addresses these characteristics.

1.1 Reversible flight control system

The flight control system of an aircraft transforms the pilot commands into aerodynamic input to the vehicle. This transformation can be accomplished by exotic fly-by-wire system or by conventional hydraulic system. They are irreversible and take advantage of the extra power available from hydraulic or electrical source as well as the advanced technology electronics to enhance the pilot capability. Mission requirements and design objective are the major drives for utilisation of these types of flight control systems. High performance commercial jets as well as fighter aircrafts usually employ such systems in which the cost is justified.

The same functions can be performed by simple push-pull rods or a combination of links and cables, which constitute the reversible flight control system. Major advantages associated with this reversible flight control systems include simplicity, which results in higher reliability, low costs, and relatively maintenance free. These advantages institute the main attraction for this type of control system for low cost commuter and general aviation aircrafts.

In addition, the reversible characteristic of this type of system has been of interest. In some cases it works to the benefit of the pilot. For instance, when stall is reached the buffeting can be used as a mean of alerting the pilot prior to the point where the actual stall is reached and the vehicle is put into a dangerous situation. In some cases, due to their simple reversible control system, they are most commonly affected by tail icing[1]. Most of the studies have concentrated on the effect of flight control system behaviour on the aircraft stability and controllability.

Another characteristic of reversible control system which employs cable as a mean of transmitting force and displacement is its nonlinearity. This nonlinear character has also been of interest and addressed when the system was being identified for implementation into the flight simulator[2,3].

It should also be recognised that some parameters of the reversible control systems such as control column displacements and forces are subjected to human limitations. Furthermore, control column force varies with the speed, trim tab position, as well as load factor[4].

Considering a longitudinal flight control system like elevator, the hinge moment is normalised with dynamic pressure, elevator area, and elevator reference cord, as:

$$HM = \tfrac{1}{2}\bar{q}_H S_E \bar{c}_E C_h \qquad \ldots (1)$$

Without listing all derivatives explicitly, the elevator hinge moment can be written as:

$$C_h = C_{h_0} + C_{h\alpha}\alpha + C_{h,\eta}\delta\eta + C_{h,\eta_{TT}}\delta\eta_{TT} + \frac{C_{h,\dot{\alpha}}\dot{\alpha}\bar{c}}{V} + \frac{C_{h,\dot{\eta}}\dot{\eta}\bar{c}}{V} + C_{h,\beta}\beta + C_{h,GE}\sigma \qquad \ldots (2)$$

By assuming an aircraft in steady level flight, the last term in the Equation (2) is omitted. Furthermore the sideslip was assumed to be zero and as a result the associated term was ignored[5]. Using Equation (2) for hinge moment coefficient, the pilot control column force can be balanced by the elevator aerodynamic hinge moment and inertial loads.

1.2 Random input loads

The known major sources affecting hinge moment characteristics are buffeting, tail ice accretion, and atmospheric turbulence.

Tail buffeting occurs when the air flow over the wing breaks down and turbulent wing wake strikes the horizontal tail. The breakdown in air flow over the wing may occur as a result of a stall[6]. Presence of the wake behind the wing is a major cause of the oscillation induced to the flow field over an aircraft tail. This random oscillation changes the loads on the horizontal tail and can be used as a mean of detecting stall in an aircraft[7]. Aviation regulations also specify that the warning can be furnished by this method[8].

Buffeting due to high angles of attack has been subject of extensive studies in the past. For instance, flight test programs were conducted to extract and use experimental data to enhance the capability of the computational fluid dynamics to predict the buffeting behaviour for practical applications[9].

Ice accretion on the tail can also change the tail aerofoil shape. In a study performed in Glen Research Centre on tail icing it was reported that the formation of ice affected the hinge moment and caused the pulsing of the control column. Flap transition accompanied with the failed boot ice showed a random oscillation of control column as the flap reached its final position[10].

Usually turbulence is considered as a stochastic process noise. Removal of atmospheric turbulence from flight data using conventional Dryden or Von-Karman model can be performed by passing a white noise through some appropriate shaping filters that generate turbulence random velocities of a given intensity and power spectra[11]. However, variation of wing and tail angle of attack due to vertical component of turbulent atmosphere is a phenomenon that can affect the hinge moment and translate into control column oscillation.

https://doi.org/10.1017/S0001924000002025 Published online by Cambridge University Press

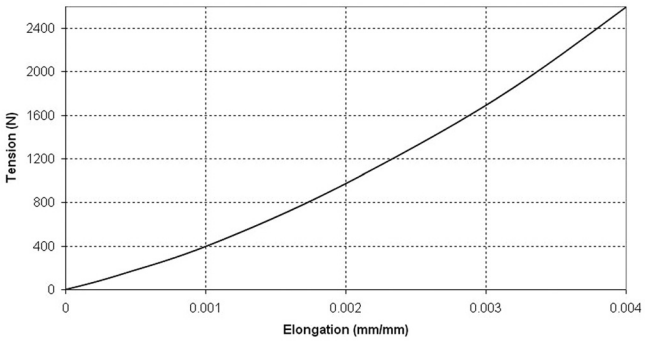


Figure 1. EA modulus of standard aviation 7×19 cable.

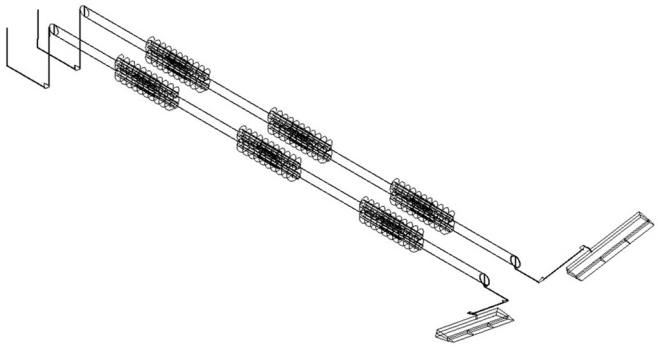


Figure 2. The full view of flight control system model.

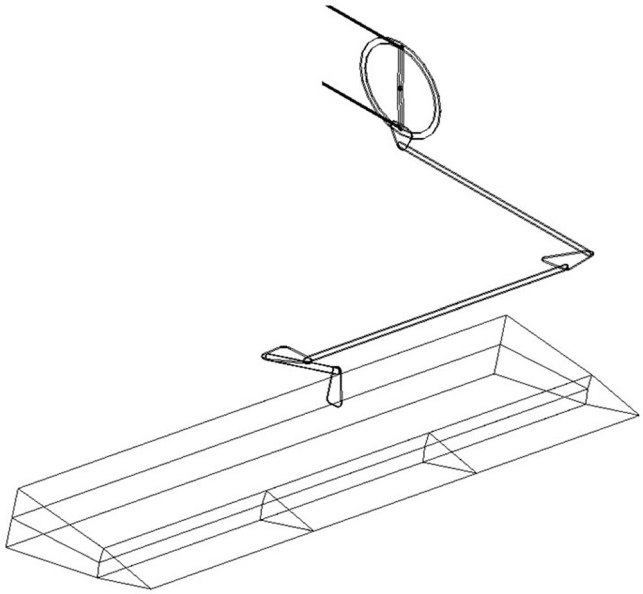


Figure 3. 3D mechanism of modelled longitudinal flight control system.

1.3 Nonlinearity in flight control system

A key element of modelling and simulation of a reversible flight control system is the nonlinear characteristics of such a system. This nonlinearity is originated by different mechanical sources like cables and friction.

Aircraft cables make an efficient means for the transmission of control loads over long distances due to their high strength and light weight. Their properties however induce many special considerations which have to be taken into account in the overall design of a flight control system. The primary modulus (EA) of the cable accounts for both the material elasticity and the stiffness of the cable construction. This constructional stiffness increases with load making the cable characteristics non-linear[3,12] (Fig. 1). It is too complex to model a control cable in detail, a methodology to mimic its effect is desirable[13].

Friction is a major cause of handling quality problems with aircrafts control system[14]. Due to nonlinearities, friction is difficult to model. Friction could be simply modelled by stick and sliding friction and neglecting viscous friction. With the respective control surface in standstill, static friction causes stiction until the external moment exceed the static friction moment. Once the control surface is in motion, there is a transition between stiction and sliding. Previous researches have indicated that the effective stick friction is zero for systems with vibration[2, 15].

For gaining an insight to the work done, we first review the modelling process in the mentioned software environment. Due to the existence of the cable as the elastic element, the frequency response of the model is discussed next. Validating the model using the recorded flight data for control column displacement in absence as well as in presence of the hinge moment is discussed. Finally, the system is excited using the severe intensity turbulent vertical velocity from Von Karman model with the same flight condition as the recorded data and the model output is then analysed.

2.0 MODELLING

A multi-body system (MBS) consists of a finite number of rigid or flexible bodies which are connected by coupling elements like joints, springs, dampers and actuators. The coupling elements are assumed to be mass-less, so that the mass of the mechanical system is concentrated in the bodies. The equations of motion of a mechanical multi-body system are given by a second order system of ordinary differential equations (ODE) as Equation (3)

$$\mathbf{M}(q)\ddot{q} = f(q,\dot{q}) \Leftrightarrow \begin{cases} \dot{q} = u \\ \dot{u} = \tilde{f}(q,u) = \mathbf{M}^{-1}(q) f(q,u) \end{cases} \quad \ldots (3)$$

If the mechanical system contains closed loops, additional algebraic constraints have to be introduced and the resulting equations of motion are given by a differential algebraic equation (DAE) that may be written in first order form as Equation (4)

$$\begin{aligned} &\dot{q} = u, \\ &\mathbf{M}(q)\dot{u} = f(q,u) - \mathbf{G}^T(q)\lambda, \\ &0 = \mathbf{g}(p) \end{aligned} \quad \ldots (4)$$

The constraint matrix $\mathbf{G}(q) = \partial \mathbf{g}(p) / \partial q$ is given by the Jacobian of $g(q)$.

It supposed that $g(q)$ has full rank to exclude redundant constraints (Grubler condition)[16].

ADAMS is a software package for the dynamic analysis of mechanical systems, implementing the multi-body technique. The user provides the description of the system in terms of the inertial properties of each rigid body, the encountered constraints and force statements modelling different kinds of point to point interactions (elastic, damping or user defined, etc.) or generic externally applied loads. This structural description is then automatically translated into a mathematical model based on above approach[17].

The reversible flight control system of the aircraft under consideration consisted of mechanical parts including forward section with control column, push-pull rods and a set of bracket, the middle part with front and rear sectors connected via cables, and the aft part with push-pull rods, brackets, elevator and trim-tabs

Figures 2 and 3, show the modelling of the system in Adams environment. The control column rod, push-pull rods, the brackets, as well as the sectors were modelled using the software basic

https://doi.org/10.1017/S0001924000002025 Published online by Cambridge University Press

Table 3
System natural frequencies

Mode	Frequency (Hz)
1	0·0966
2	25·073

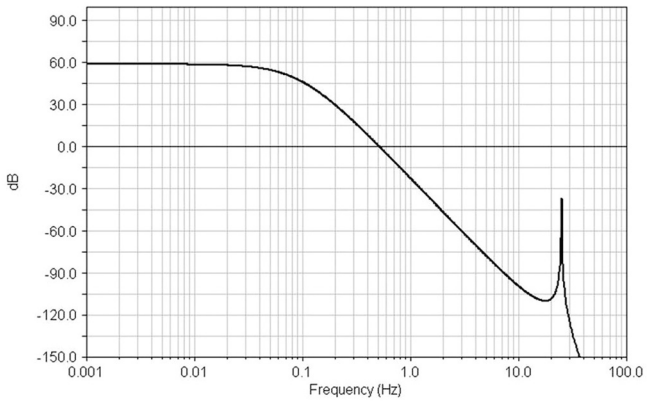


Figure 4. Power spectral density of control column displacement.

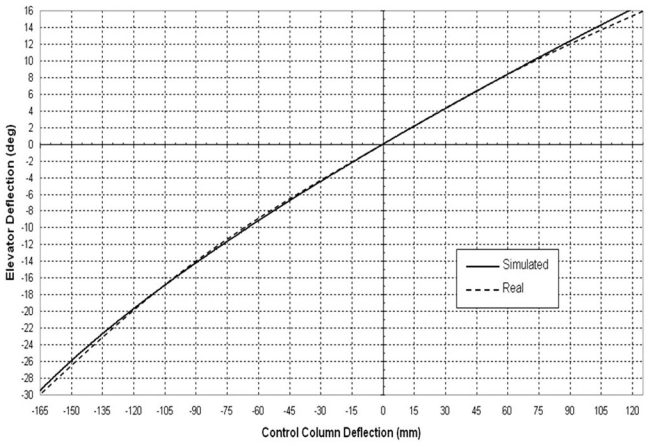


Figure 5. Kinematical characteristics comparison.

elements. The cables were modelled using the mass in form of solid rods and stiff springs.

For completeness of modelling, all mass properties of parts such as mass, moment of inertia, and centre of gravity locations were considered. This was of utmost importance for the cables since a unique feature of this modelling was the inclusion of mass in the cable model.

The above mentioned parts are constrained by the variety type of predefined joints like revolute, hook, transitional and primitives. The cables and the sectors are coupled by gear joints[3].

Friction is modelled based on information which was obtained using Boeing design method[18]. According to oscillatory behaviour of nonlinear dynamic input loads, just sliding friction is taken into account by $\mu = 0{\cdot}04$.

Cables are modelled by an aviation standard 7×19 cable[19]. It was modelled considering other conventional method[3,13,20-22] as a set of stiff springs and the plenty of cylindrical solids which represent mass properties of cables.

For validating the cable model the equation of nth order natural frequency f_n of a taut string is used[12] as Equation (5) and was

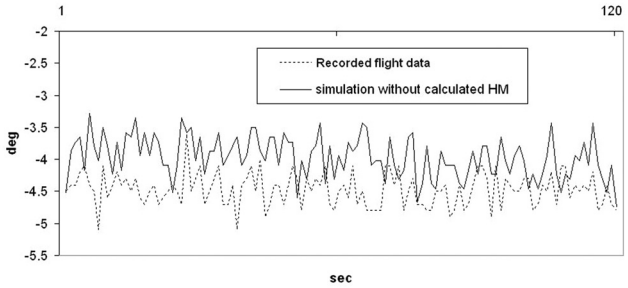


Figure 6. Elevator deflection, considering only inertial forces and friction for flight #1.

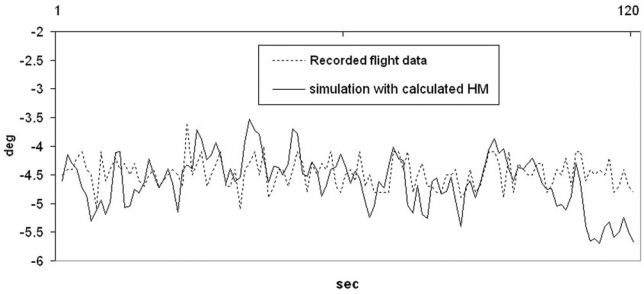


Figure 7. Elevator deflection, adding aerodynamic hinge moment for flight #1.

compared successfully with the modelled cable in ADAMS.

$$f_n = \left(\frac{n}{2l}\right)\sqrt{\frac{T}{m}} \qquad \ldots (5)$$

3.0 MODEL FREQUENCY ANALYSIS

Since the model employed some elements that have elastic properties and the system was going to be subjected to time varying inputs, a frequency investigation of the system was essential. As a result, the software vibration tool was used to shake the elevator using swept sine method and the control column displacement and acceleration response was recorded. Fundamental rigid body natural frequency appears on lower end of the spectrum at 0·0966Hz (Table 3 and Fig. 4).

4.0 MODEL VALIDATION

The model validation was performed in two steps; First, the time invariant check of the displacements and second the time variation using recorded flight data for the elevator and control column.

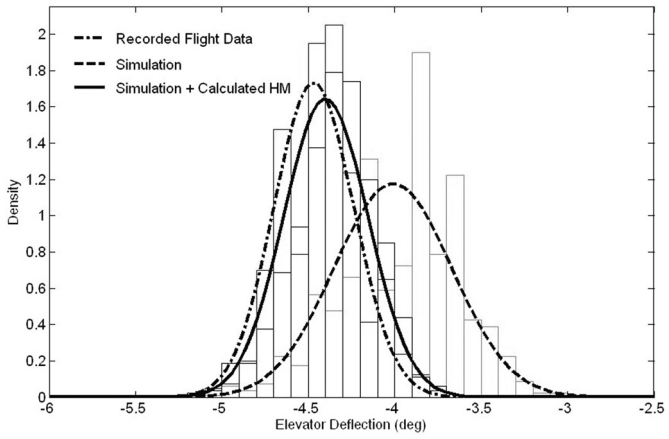
4.1 Time invariant

The characteristic of kinematical connection between control column and elevator can be stated as Equation (6)

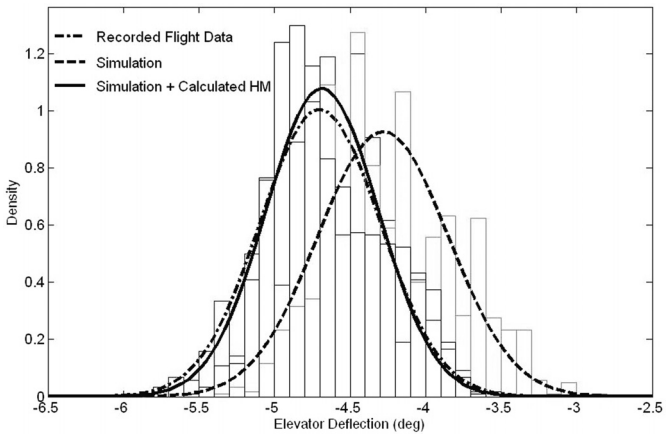
$$\eta = f\left(X_n\right) \qquad \ldots (6)$$

The kinematical simulation of constructed model was performed and compared by considered aircraft as Fig. 5. This graph shows that the relationship is somehow nonlinear.

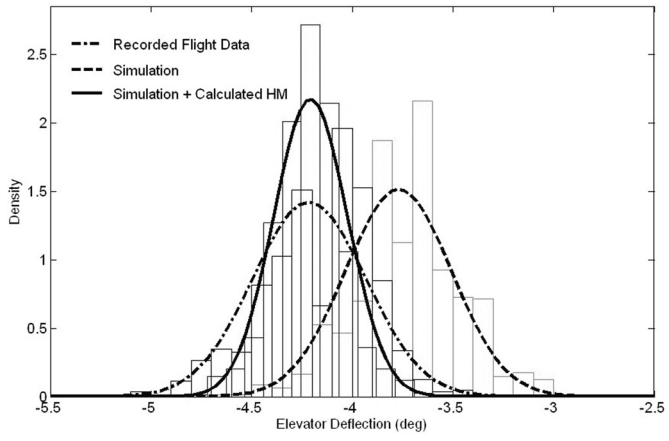
https://doi.org/10.1017/S0001924000002025 Published online by Cambridge University Press



(a)



(b)



(c)

Figure 8. Probably density function of elevator deflection (a) Flight #1 (b) Flight #2 (c) Flight #3.

4.2 Time varying

For checking the system response to a time varying input, the flight recorded data for two minutes steady flight was compared to the simulation results in two scenarios. For the first case the hinge moment was not taken into account which resulted in a difference with the recorded data. For the second case a hinge moment was calculated using the time history of tail angle of attack, elevator and trim tab deflection along HM derivatives. The results as shown in Figs 6 and 7 indicate proper estimation of HM.

For stochastic analysis of the results, three sets of recorded flight data, mentioned in Table 2, were used. Each recorded file contained data from take off to landing. Only the level flight segments were chosen.

For each flight two sets of elevator data existed; one from flight and one from the simulation. Probability density of each set revealed a mean which would differ as in Fig 6. Addition of the calculated hinge moment would reduce this difference.

Figure 8 shows probability distribution function of elevator deflection from the analysis performed on the three flights and their associated elevator deflection from flight. Addition of hinge moment in this figure caused the mean for the simulation to move closer to elevator mean value from flight. Closeness of the simulation and recorded elevator deflection validates the modelling and hinge moment calculations (see Table 4).

Table 4
Statistical comparison of elevator deflections Flight (R) and Simulation (HM included) (S)

Flight	Data	Mean	Variance
1	R	–4·46	0·0529
	S	–4·39	0·0580
2	R	–4·69	0·157
	S	–4·68	0·136
3	R	–4·21	0·078
	S	–4·20	0·033

5.0 EXCITATION WITH RANDOM INPUT

All flights encounter some kind of turbulence depending on region of the Earth, season of the year as well as flight altitude. It has been associated with both clouds and clear air (CAT). Intensity level can be light, moderate, or severe depending on the magnitude of the vertical velocities involved.

Based on weather reports, pilots always try to avoid turbulent weather altogether by changing direction or altitude and placing the aircraft in smooth air.

However, this is not always possible. In such case angle of attack changes rapidly and in a random manner. This causes a change in flow field around the tail which results in variation of the hinge moment as well. Due to the reversible nature of a flight control system, hinge moment variation can force the control column to oscillate.

For the flight under consideration, the turbulence was extracted using the wind-based method for the three flight conditions mentioned in Table 2.

For this purpose the vertical velocity of the centre of mass and the component of the aircraft velocity were used to calculate the turbulent vertical velocity according to Equation (7)[5].

$$w = \dot{Z} + V[\mathrm{Cos}(\phi)\mathrm{Sin}(\alpha)\mathrm{Cos}(\theta) - \mathrm{Cos}(\alpha)\mathrm{Sin}(\theta)] \quad \ldots (7)$$

Based on the analysis of recorded data and their comparison with Von Karman model, it was concluded that all flights encountered only light turbulence, as shown in Fig. 9.

In addition, the investigation of the dynamic phenomena and sensor used for data collection revealed the clear distinction between the measured noise and atmospheric turbulence effect.

Addition of the turbulence with a severe intensity level, as random input to the model, could give an insight to its behaviour. For this purpose a von Karman model was used to generate vertical

https://doi.org/10.1017/S0001924000002025 Published online by Cambridge University Press

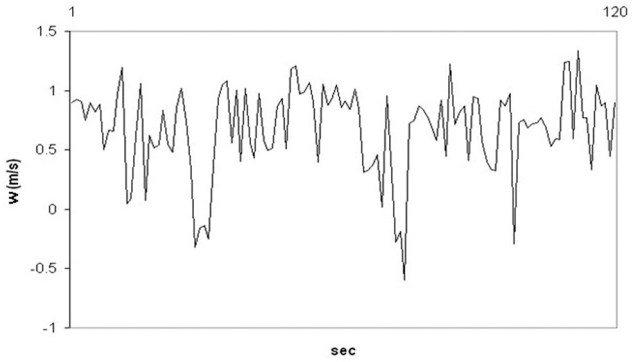


Figure 9. Turbulence vertical velocity extracted from recorded flight data.

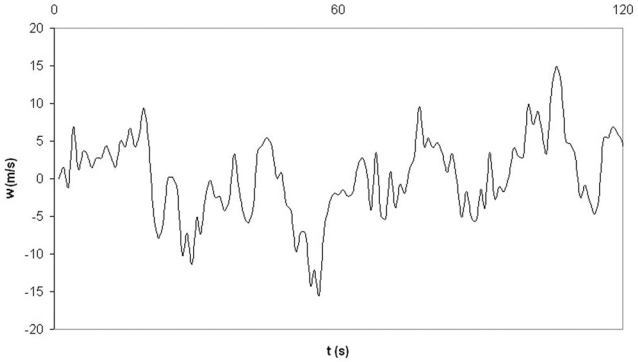


Figure 10. Time history of generated turbulence vertical velocity.

component of turbulence for the same flight condition (Fig. 10). The vertical velocities were then converted to the change in tail angles of attack and used for calculation of the hinge-moments. By applying these hinge-moments to the elevator in the model, the changes of control column forces were simulated.

Figure 11 shows the power spectral density of the turbulence from the three flights and the output of the Von Karman model based on the similar flight condition.

6.0 RESULTS

The system under consideration contains two nonlinear elements; namely the nonlinear cable and coulomb friction. Both elements affect the peak at 25Hz which is far above the frequency regions where the turbulence affects the system. As a result using a linear model would suffice for the analysis at hand.

For comparing the frequency modes for the cable model in the Adams software with that of Equation (5), a separate model was developed. The same preload was placed on the cable and vibration simulation was performed on it. Since three springs were used to represent the cable, only the first two modes were extracted. They showed good agreement with those calculated from taut string formula, as shown in Table 5. This indicated that modelling of cable with spring and mass is valid and its usage for further analysis was appropriate.

The power spectral density of the HM based on the associated derivatives for the aircraft under consideration and recorded time history of elevator and trim tab deflections as well as the angle-of-attack is shown in Fig. 12.

Adjusting the tail angle of attack to include the effect of vertical component of turbulence velocity, the power spectral density of HM takes the form of Fig. 13.

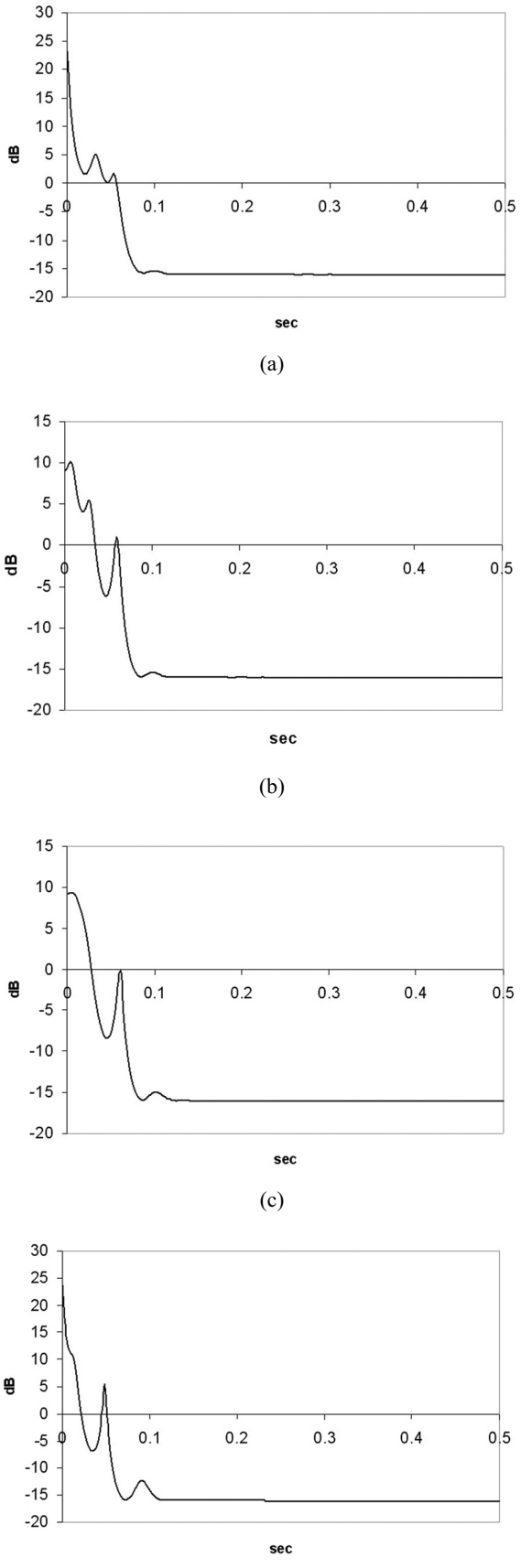


Figure 11. Power spectral density of generated turbulence vertical velocity. (a) Flight #1 (b) Flight #2 (c) Flight #3 d) von Karman model.

https://doi.org/10.1017/S0001924000002025 Published online by Cambridge University Press

Table 5
Comparison of cable natural frequency (Hz) from ADAMS software model with taut string formula

Mode	Adams	Taut string theory	% error
1	1·07	1·006	6·36
2	2·005	2·01	0·34

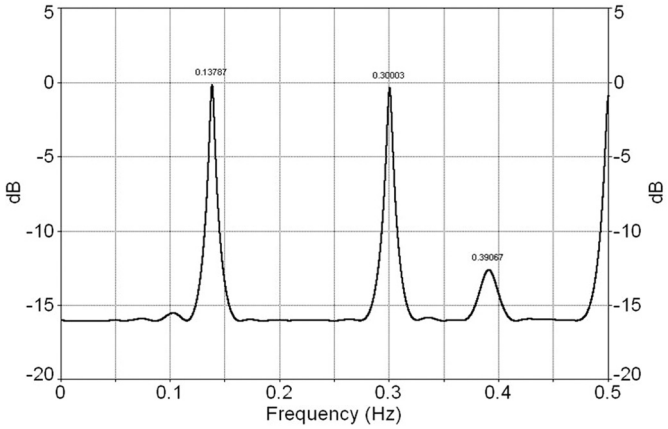


Figure 12. Power spectral density of HM.

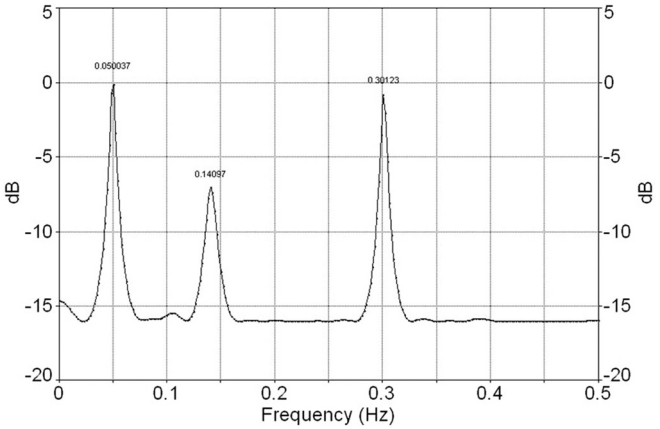


Figure 13. Power spectral density of HM with turbulence.

As Fig. 13 shows, the energy in severe turbulence resulted in a new mode at about 0·05Hz. The HM containing turbulence effect was implemented in the model as input, while the displacement and the acceleration of the control column were taken as the output The results are shown in Fig.14.

The model output shows that when an aeroplane is subject to severe turbulence, the vertical component of the turbulence affects the hinge moment around 0·05Hz and this in turn is transmitted to the control column due to the reversibility of the flight control system Fig. 15 shows the displacement of the control column associated with the above low frequency mode.

7.0 CONCLUSION

Upon examination of the results, it can be seen that turbulence can act as a random input through the hinge moment during the flight and introduce a new mode in the lower end of power spectral density curve. This low frequency input induces some energy to the flight control. However due to its nature, it cannot exert large forces to the pilot or movements beyond its reaction time. Yet the simulation showed that it can cause large displacement of control column which surpassed the existing limits. Therefore it should be taken into account when dealing with handling quality as well as autopilot design.

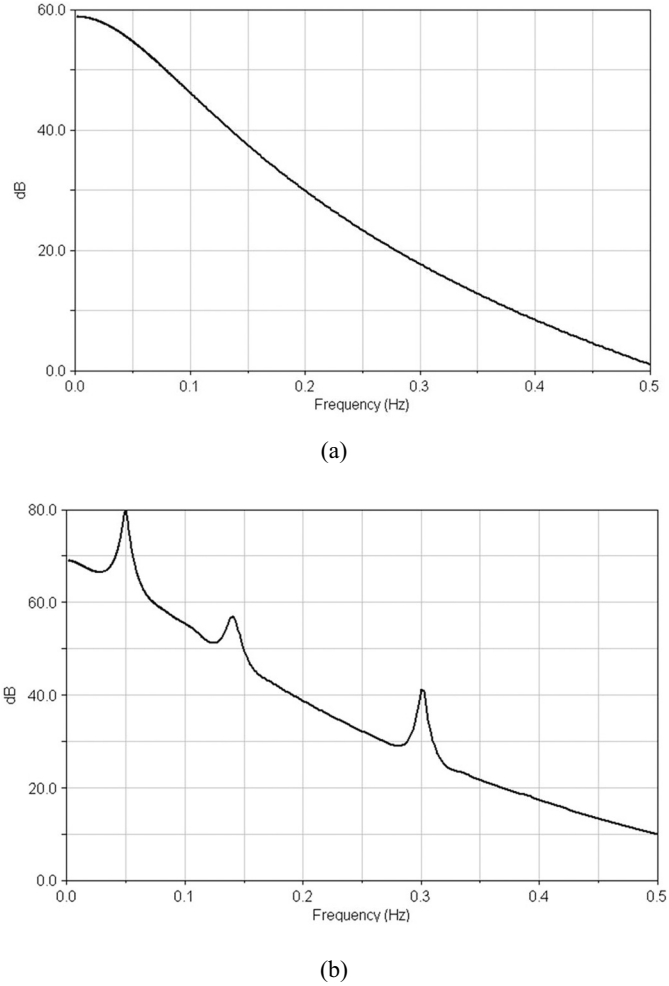


Figure 14. Power spectral density of control column displacement
(a) Prior to implementation of turbulence
(b) After implementation of turbulence.

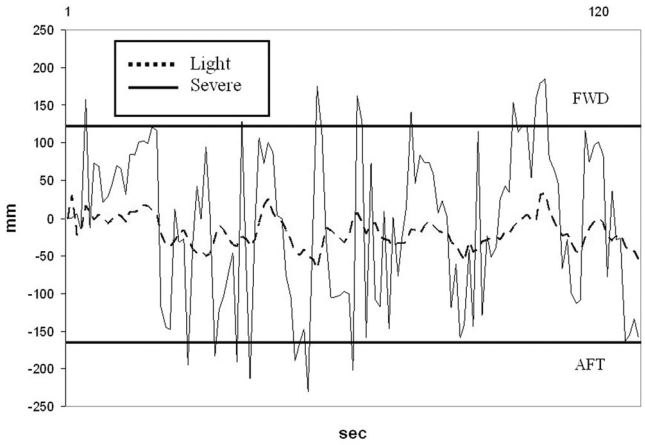


Figure 15. Control column displacements for light and severe turbulence bounded by the most aft and fwd limits of movement.

https://doi.org/10.1017/S0001924000002025 Published online by Cambridge University Press

Further investigation of this phenomenon can give a better understanding into the behaviour of such systems during turbulence encounter in general and especially when coupled with other existent phenomenon such as buffeting. The overall result can enhance the safety for this class of aircrafts which incorporate reversible flight control system.

REFERENCES

1. HILTNER, D.W. An evaluation of an analytical simulation of an airplane with tailplane icing by comparison to flight data, 2000, NASA/CR-2000-210561, Glen Research Center, Ohio.
2. WEISS, S., GOCKEL, W., MONNICH, W. and ROHLF, D. Identification of Dornier-328 reversible flight control system, 1998, AIAA Modeling and Simulation Technology Conference, Boston, MA, August 1998.
3. GODIN, F.R. Aircraft flight control system modelling — cable construction kit, 2000, International ADAMS User Conference, Orlando, Florida, 19-21 June 2000.
4. ROSKAM, J. Airplane flight dynamics and automatic flight control, 1998, Roskam Aviation Corporation, Ottawa, Kansas.
5. CORNMAN, L.B. MEYMARIS, G. and LIMBER, M. An update on the FAA aviation weather research program's in situ turbulence measurement and reporting system, 2004, National Center for Atmospheric Research, Boulder, Colorado, US.
6. GOODMAN, H.R. Over-all loads and buffeting measurements, 1948, Air Force — NACA Conference, Muroc Air Force Base, CA.
7. SADOFF, M. AND SISK, T. Stall characteristics obtained from Flight 10 of Northrop X-4 No 2 airplane, 1950, NACA Research Memorandum, Washington.
8. ANON Federal Aviation Regulation 25.207, 2001, Federal Aviation Administration, Washington.
9. SHARMA, V.K. P-3 Aircraft buffet response characterization, 2001, 39th Aerospace Science Meeting and Exhibition, Reno, NV, January 2001.
10. RANAUDO, R.J., RATVSAKY, T.P. and VAN ZANTE, J.F. Flying qualities evaluation of a commuter aircraft with an ice contaminated tailplane, 2000, SAE General Aviation Technology Conference, Wichita, KS.
11. JATEGAONKAR, R. Flight vehicle system identification, *AIAA Progress in Astronautics and Aeronautics*, 2006, **216**, Reston, VA.
12. WEI-XIN R., GANG C. and WEI-HUA, H. Empirical formulas to estimate cable tension by cable fundamental frequency, *Structural Engineering and Mech*, 2005, **20**, (3), pp 363-380.
13. PARK, J. ADAMS Modeling technique for mechanical control cables, 2001 ADAMS User Conference at Novi Hilton, Michigan, USA.
14. ROSKAM, J. *Airplane Design Handbook*, Roskam Aviation Corporation, Ottawa, Kansas, 1979.
15. CHECK, K.C., HU, H. and LOH, N.K. Modeling and identification of a class of servomechanism systems with stick-slip friction, *J Dynamic Systems*, *Measurement and Control*, 1988, **110**, pp 324-328.
16. BURGERMEISTER, B., ARNOLD, M. and ESTERL, B. DAE time integration for real-time applications in multi-body dynamics, *J Applied Mathematics and Mech*, 2006, **86**, (10), pp 759-771, Wiley-VCH Verlag, Weinheim.
17. BERTOGALLI, V., BITTANTI, S. and LOVERA, M. Simulation and identification of helicopter rotor dynamics using a general-purpose multi-body code, *J of The Franklin Institute*, 1999, **336**, pp 783-797.
18. ANON Boeing design manual — mechanical control — cable friction, 1978, Boeing Co.
19. ANON General specification for wire rope, flexible, for aircraft control, April 2005, MIL-DTL-83420M.
20. SLAGOWSKI, S. and POTTER, A. Using ADAMS to model cable driven hyper-redundant flexible manipulators, 2000 International ADAMS User Conference.
21. ELLIOTT, A.S. Efficient modeling of extensible cables and pulley systems in ADAMS, 2002 European ADAMS Users Conference.
22. ANON. Modeling and simulating process, 2002, ADAMS/Solver Documentation.

https://doi.org/10.1017/S0001924000002025 Published online by Cambridge University Press